Stochastic surface-based modeling of turbidite lobes

Michael J. Pyrcz, Octavian Catuneanu, and Clayton V. Deutsch

ABSTRACT

Flow event deposits in turbidite lobes are modeled with stochastic surface-based simulation. This method honors the geometries and compensational stacking of flow event deposits. Flow event deposit geometries are based on a flexible lobe parameterization. Compensational stacking is the tendency of flow event deposits to fill topographic lows and to smoothing of topographic relief. The surface-based model may be conditioned to well data.

Models of reservoir properties such as porosity and permeability are constrained by the resulting geometric models. This approach is applied in a geostatistical workflow to better integrate available geologic information. The resulting models may improve the accuracy of model reservoir response and account for the uncertainty in the heterogeneity of turbidite lobes.

INTRODUCTION

The inaccessibility of the subsurface generally results in a high degree of uncertainty. Stochastic models provide a measure of uncertainty in reservoir response through the construction of multiple realizations of lithofacies, porosity, and permeability. Stochastic models are commonly cell based; the model is constructed on a by-cell basis. These models are generally limited to the reproduction of two-point statistics, the semivariogram, and do not reproduce complicated spatial structures. The desire to construct more geologically realistic stochastic models has led to research in object-based and surface-based models. Object-based or Boolean techniques were pioneered by Haldorsen and Lake (1984), Haldorsen and Chang (1986), and Stoyan et al. (1987). Surface-based techniques have been introduced recently (Deutsch et al., 2001; Pyrcz and Deutsch, 2003).

With turbidite systems as important exploration targets, there has been a rapid increase in exploration in both convergent and passive margins in the last 20–30 yr (Stow and Mayall, 2000). There

Manuscript received October 8, 2003; provisional acceptance January 8, 2004; revised manuscript received September 11, 2004; final acceptance September 22, 2004.
DOI:10.1306/09220403112

AUTHORS

Michael J. Pyrcz ~ *Quantitative Stratigraphy, ChevronTexaco Energy Technology Company, 4800 Fournace Place, Bellaire, Texas 77401; mjpy@chevrontexaco.com*

Michael Pyrcz has just completed a Ph.D. at the School of Mining and Petroleum Engineering, Department of Civil and Environmental Engineering at the University of Alberta and has recently been hired by ChevronTexaco. Pyrcz has published several peer-reviewed technical papers and five papers in conference proceedings and has written a variety of geostatistical algorithms for deepwater and fluvial depositional settings.

Octavian Catuneanu ~ *Department of Earth and Atmospheric Sciences, University of Alberta, 1–26 Earth Sciences Building, Edmonton, Alberta, Canada T6G 2E3; octavian@ualberta.ca*

Octavian Catuneanu is professor in the Department of Earth and Atmospheric Sciences at the University of Alberta, with a Ph.D. in geology from the University of Toronto. He is the recipient of a 2002 Best Paper Award of the Geological Society of America and a specialist in sedimentology, stratigraphy, and basin analysis. Catuneanu is the chair of the Canadian Sedimentology Research Group and a member of the North American and European Commission on Stratigraphic Nomenclature and Classification. He is the author of two textbooks and over 50 full-length, peer–reviewed research and review articles and editor of several books and special volumes. Catuneanu is involved in a number of international research programs and is an instructor of sequence stratigraphy for conferences and companies from around the world.

Clayton V. Deutsch ~ *Department of Civil and Environmental Engineering, University of Alberta, 220 CEB Building, Edmonton, Alberta, Canada T6G 2E3; cdeutsch@ualberta.ca*

Clayton Deutsch is a professor in the School of Mining and Petroleum Engineering, Department of Civil and Environmental Engineering at the University of Alberta. He teaches and conducts research into better ways to model heterogeneity and uncertainty in

petroleum reservoirs. Deutsch has published 2 books, more than 70 peer-reviewed technical papers, and more than 70 papers in conference proceedings.

ACKNOWLEDGEMENTS

We acknowledge the industrial supporters of the Center for Computational Geostatistics at the University of Alberta, the National Science and Engineering Research Council of Canada, and the Informatics Circle of Research Excellence in Alberta.

is a great deal of research into the internal and external geometries and stacking patterns of architectural elements associated with turbidites (Satur et al., 2000; Shanmugam, 2000; Stow and Johansson, 2000; Stow and Mayall, 2000; Johnson et al., 2001). A classification scheme based on grain size and feeder system has been developed to describe various architectural element associations (Reading and Richards, 1994; Bouma, 2000). Ghosh and Lowe (1993) constructed a hierarchy of process-based architectural elements, and Pickering et al. (1995) presented a scheme focused on internal and external geometry.

The Ghosh and Lowe (1993) scheme is applied in this paper. Individual homogeneous components are identified as first-order architectural elements. These may be individual components of the Bouma sequence ($T_{\mathrm{a-e}}$) and other coarser components (Bouma, 1962). The second-order architectural elements are composed of a single or collections of first-order elements that represent products of individual flow events. Third- and fourth-order architectural elements represent reservoir-scale features such as lobes or channel-levee systems.

Small-Scale Geometries

Small-scale geometries are represented by first- and second-order architectural elements (Ghosh and Lowe, 1993). These elements have a thickness of less than 1 m (3.3 ft) to a few meters and are generally below the resolvable limit of seismic data but may impose significant control on the reservoir response (Slatt et al., 1998; Satur et al., 2000). These elements are referred to as flow event deposits in this paper.

The flow event deposits (1) are below the resolution of available data in the interwell regions; (2) have geometries that may be generalized with site information and analog information with the aid of an understanding of the sedimentary processes; (3) commonly have compensational stacking patterns; and (4) may have a significant impact on reservoir response.

Well tests, seismic data, and well logs commonly provide excellent structural and stratigraphic information but do not adequately resolve these small-scale features in the interwell regions. Analog outcrop studies may provide information about the character of these features. Turbidite lobe reservoir models should account for this information for improved geologic realism of the resulting reservoir models.

Stow and Johansson (2000) noted that the small-scale geometries commonly mimic the larger scale geometry. A lobe may be filled by flow event deposits with lobe geometry and compensational stacking.

Compensation cycles are defined as a main characteristic of ancient lobes (Mutti and Normark, 1987; Mutti and Normark, 1991; Galloway and Hobday, 1996; Stow et al., 1996) and are considered virtually ubiquitous in distal lobes (Mutti and Sonnino, 1981). These cycles are the result of preferential filling of topographic

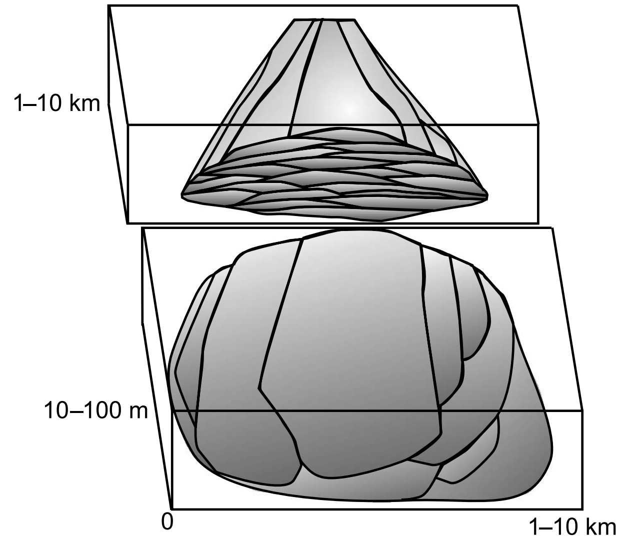

Figure 1. The morphologies reproduced with the surface-based model. The figure includes a single turbidite lobe filled by flow event deposits with compensational stacking. This geometric model may be applied to constrain reservoir-quality trends and to position mud drapes along the surfaces. Trends in flow events may include fining upward, distal, and toward the peripheries.

lows. In vertical profile, compensational cycles are identified as multiple thickening-upward sequences. A schematic of the geometries reproduced in the surface-based turbidite lobe model is shown in Figure 1.

Petrophysical property distributions may be constrained by trends related to these small-scale features. In addition, in mud-rich and mud-sand-rich systems, stochastic mud drape models may be positioned along the stochastic surfaces (similar to Li and White, 2003). Associated features may result in geologic barriers and baffles to flow and may have a significant impact on oil and gas production.

A stochastic surface-based simulation approach is introduced for modeling the geometry of flow event deposits in turbidite lobes. This method honors the geometries and compensational stacking between the flow event deposits. These flow event deposit geometries are based on a flexible lobe parameterization (Figures 2, 3). Further discussion of the methods presented in this paper and the required algorithms are provided in Pyrcz (2004).

Large-Scale Geometries

The large-scale sand bodies in distal deepwater clastics have been characterized as massive sand facies associations by Stow and Johansson (2000) and are classified as third- and fourth-order architectural elements by Ghosh and Lowe (1993). They include reservoir-scale lobes (Stow and Johansson, 2000) and may be correlated in well log and characterized by seismic survey. These architectural elements are referred to as lobes in this paper.

Discussion on Data

Without the data, there would be little difficulty in reproducing the complicated geometries in a depositional setting. Quantitative dynamic stratigraphy models based on initial and boundary conditions and on a continuum of relationships spanning well-established fundamental laws, first-order approximations, and empirical relationships to poorly defined gross empirical relationships are available (Cross and Harbaugh, 1990). These models are able to reproduce many of the geometries and relationships observed in the rock record.

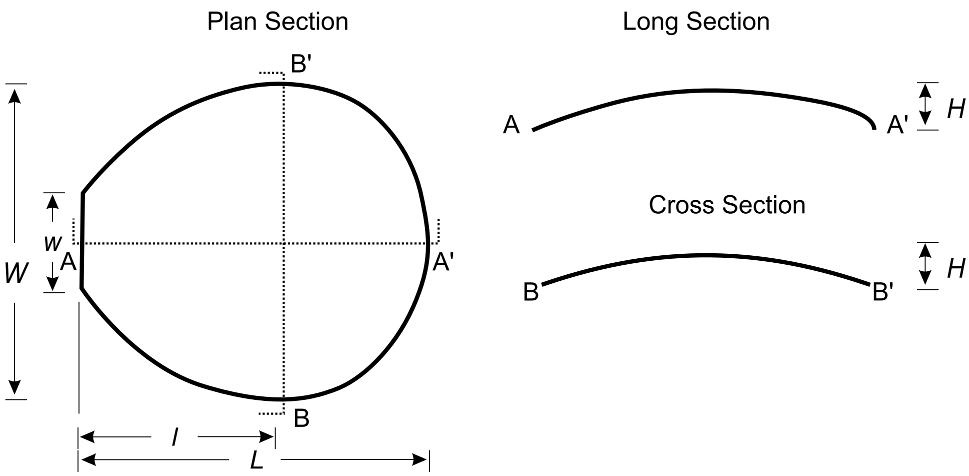

Figure 2. The flow event geometry and associated parameters. Note that this geometry is fit to a curvilinear axis of flow and is modified by a stochastic residual. These operations remove the unrealistic regularity and result in a flexible geometry with low to high sinuosity and lobe, linguoidal and ellipsoid morphologies.

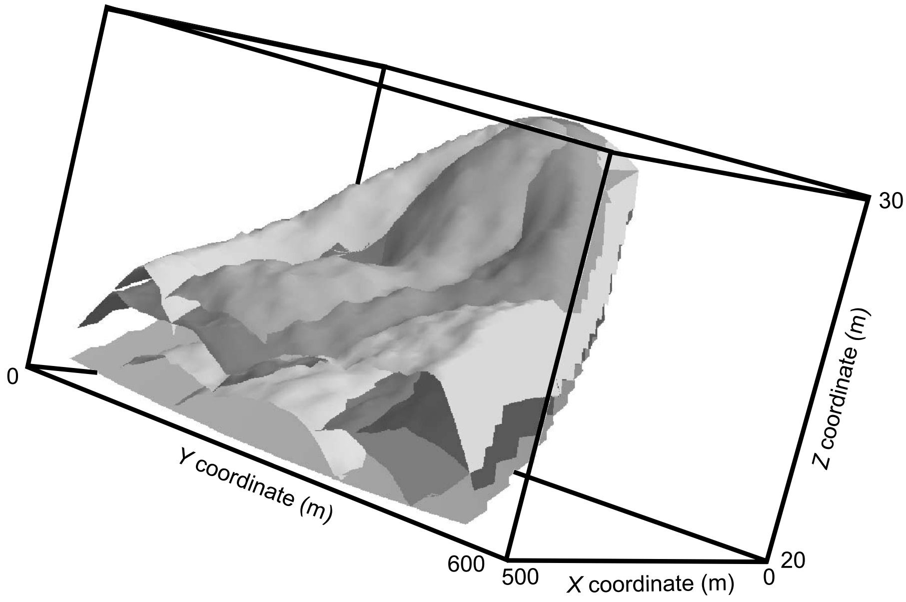

Figure 3. An example surface-based simulation of flow event deposits with lobe geometries. The surfaces are cut to reveal the compensational stacking pattern.

Although quantitative dynamic stratigraphy models are useful for refining conceptual models, their chaotic nature renders them unable to integrate local conditioning, such as from well logs and cores and seismic survey. Solving for appropriate initial and boundary conditions to honor site-specific conditioning is an intractable inverse problem. Iterative pseudoinverse modeling approaches are not feasible given the computational requirements of quantitative dynamic stratigraphy models. In addition, quantitative dynamic stratigraphy models do not efficiently provide a measure of uncertainty.

Geostatistical methods are able to reproduce various levels of geometric complexity while allowing for conditioning to a variety of site-specific data. Pixel-based methods, such as sequential indicator simulation and truncated Gaussian simulation, may be applied to construct stochastic facies models that reproduce spatial structures limited to the semivariogram (Alabert and Massonnat, 1990). Multiple-point geostatistics have been applied to reproduce curvilinear features in deepwater settings (Strebelle and Payrazyan, 2002). The fluvial simulation (FLUVSIM) (Deutsch and Tran, 2002) object-based fluvial model has been modified to reproduce submarine channels with attached lobes. However, these models may not integrate geologic information with regard to flow event geometries and stacking patterns. A surface-based turbidite lobe algorithm is described and demonstrated in a geostatistical workflow on an example outcrop. This approach may be applied to lobes in mud-rich, mud-sand-rich, and sand-rich systems with single or multiple sources. The resulting geometric models may be applied to constrain trends in reservoir quality.

METHODOLOGY

Reservoir-scale lobe geometry is established from available data. A measurement of uncertainty is assigned based on data accuracy, so that this uncertainty may be accounted for as simulated fluctuations in the reservoir geometry. The lobe geometry defines the original bathymetry and the reservoir extents.

The algorithm proceeds by generating stochastic flow event deposits defined by stochastic bounding surfaces. These flow event deposits have geometries based on parameter distributions from available site and analog information. The calculation of the stochastic flow events requires two steps. First, the geometry is generated, and then a stochastic residual is added. The geometric construction considers factors such as (1) source location, (2) bathymetry, (3) flow path, and (4) characteristic geometry. The stochastic residual accounts for fluctuations in the bounding surfaces and is conditioned to well data.

The source location represents the entry location of a flow event into the lobe, where a feeding channel loses its confined character. The source is stochastically located along the proximal margin of the lobe prior to each flow event. The source location is drawn

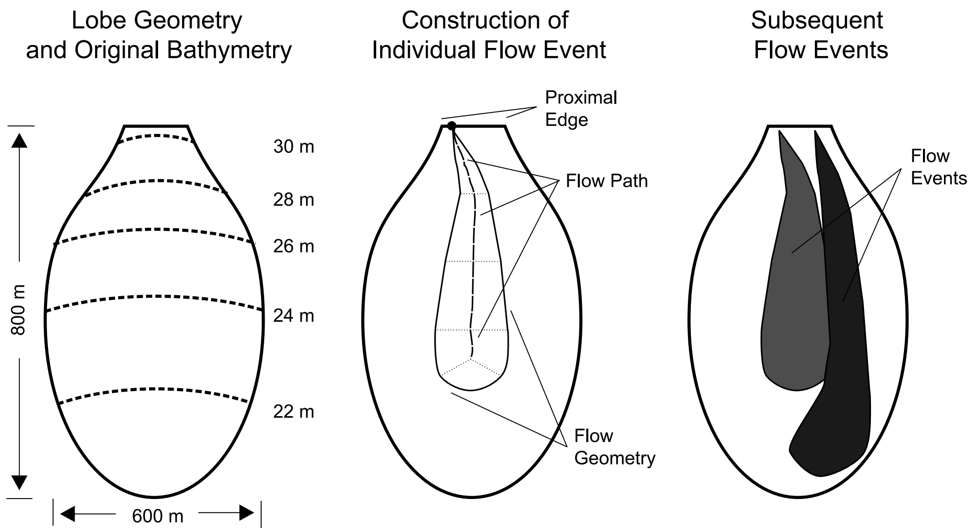

Figure 4. The construction of individual flow event deposits in a lobe. An example lobe geometry and bathymetry are defined. Stochastic flow events are generated, characterized by flow path and flow geometry. Flow events modify topography, and topography influences the position of subsequent flow events.

from a probability distribution, with the probability inversely proportional to the elevation of the margin, and flow events are more likely to enter in the lowest parts of the proximal margin of the lobe.

The bathymetry is initialized as the base of the lobe. Subsequent flow events modify this bathymetry, which affects the path of subsequent flow events. Flow paths are set to follow the path of steepest gradient. The length of the flow path is based on a stochastically drawn flow event deposit size. See Figure 4 for a schematic illustrating the construction of the geometry of individual flow event deposits in a lobe.

Nominal amplitude and a semivariogram model characterize the stochastic residual. The semivariogram model defines the smoothness of this residual. The residual is simulated by a two-dimensional version of sequential Gaussian simulation from the geostatistical library (Deutsch and Journel, 1998).

The sequential Gaussian simulation realization is conditioned to neighboring well data, as demonstrated in Figure 5. If the surface geometry contradicts data outside a tolerance, then the geometry is rejected and recalculated. The algorithm terminates when the container is entirely filled.

Trends

Reservoir property trend models constrained to the surface-based model of flow event deposits in a reservoir-scale lobe are calculated. These trend models, with respect to the flow events and lobes, are then incorporated into the stochastic property models. Because these

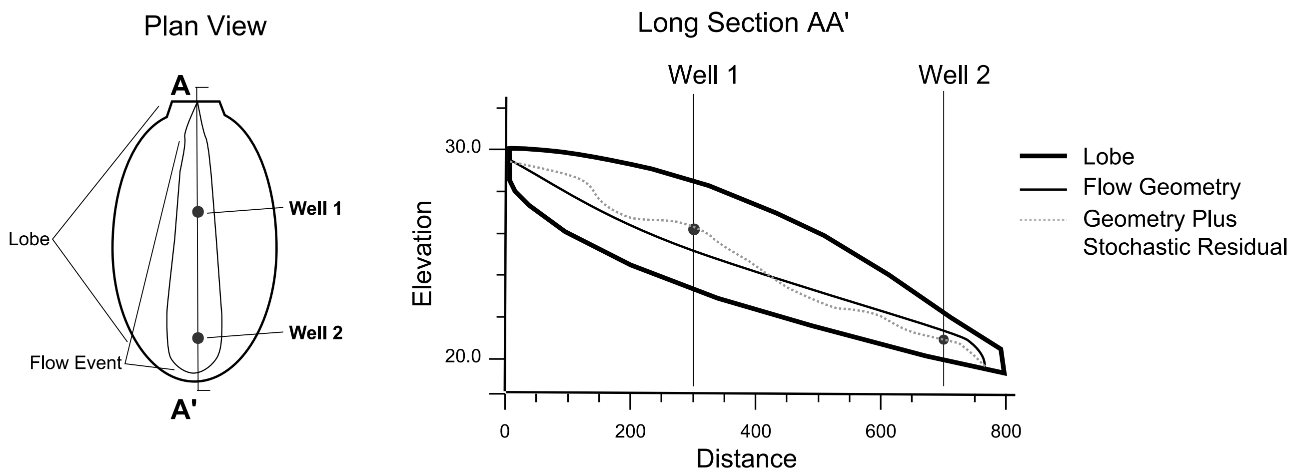

Figure 5. The addition of a stochastic residual to characterize fluctuations and to allow for conditioning to well data. For demonstration purposes, two wells are shown with a single contact on each identified as a second-order surface. Note that the stochastic surface honors the flow event deposit geometry, the well contacts, and the expected undulation.

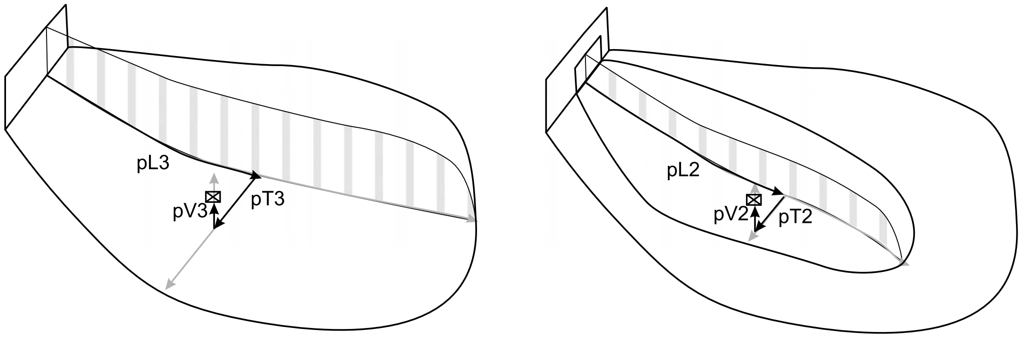

Figure 6. An illustration of the coordinate system describing vertical, longitudinal, and transverse location in nested architectural elements (left at lobe scale and right at flow event scale). The striped section represents primary flow axis at each scale. pV3, pT3, and pL3 represent the proportional coordinates in the lobe, and pV2, pT2, and pL2 represent the proportional coordinates in a flow event deposit.

trend models account for trends of a variety of hierarchies, they are subsequently denoted as hierarchical trend models (Pyrcz, 2004). A hierarchical trend model is calculated with the following steps. (1) The trend model is quantified by functions at each scale and in the principal directions relative to the flow axis: vertical from the bottom to the top of architectural elements, longitudinal from proximal to distal along the primary axes, and transverse orthogonal from the primary axes to the termination of the architectural elements (Figure 6). (2) The local trend multipliers at each location are calculated based on the relative location and specified trend functions. (3) A composite trend model is calculated by scaling the property average by the local trend multipliers (equation 1).

$$\text{trend}(\mathbf{u}) = \overline{\phi} \cdot V3(\mathbf{u}) \cdot V2(\mathbf{u}) \cdot L3(\mathbf{u}) \cdot L2(\mathbf{u}) \cdot T2(\mathbf{u}) \cdot T3(\mathbf{u}) \tag{1}$$

where $\mathbf{u}$ is a location vector, $\overline{\phi}$ is the property average, and $V3(\mathbf{u})$, $V2(\mathbf{u})$, $L3(\mathbf{u})$, $L2(\mathbf{u})$, $T2(\mathbf{u})$, and $T3(\mathbf{u})$ are the local trend multipliers. This method of combining the trend multipliers is based on the assumption of conditional independence and may not be suitable for all settings. For example, if the location $\mathbf{u}$ is at the top of a flow event deposit, the multiplier $V2(\mathbf{u})$ may be close to 0.0 if mud drapes are present. This will have a dominant impact on the resulting trend value at location $\mathbf{u}$.

The final trend model is standardized to ensure that the global mean is correct and the variance or level of variability described by the trend model is appropriate (see Isaaks and Srivastava, 1989; Deutsch, 2002, for discussion on the decomposition of trend and residual). Large-scale conditioning from seismic and well test is integrated by a posteriori correction of the areal and vertical trend in the hierarchical trend model.

CASE STUDY

A synthetic case study was constructed approximately based on outcrop studies of lobe VII of the Cengio turbidite system (Italy) of the Tertiary Piedmont basin (Cazzolo et al., 1985). Lobe VII is dominated by compensational cycles that constrain the distribution of lithofacies. Many other well-studied modern and ancient examples contain significant compensational cycles, including Mississippi middle Miocene (M4) (De Vay et al., 2000), Gottero turbidite system, Italy (Nilsen and Abbate, 1985), and Tanqua Karoo subbasin, South Africa (Dudley et. al, 2000). The Cengio turbidite system is comprised of eight tabular lobes with thickness ranging between 5 and 25 m (16 and 82 ft). Lobe VII is roughly 20 m (66 ft) thick and extends for about 6 km (3.6 mi) and is bounded on the west to north by a slope mudstone.

Subsequent flow event deposits may be separated by mud drapes and have persistent internal lithofacies trends. The mudstone facies are thinly bedded and are not laterally persistent (Cazzolo et al., 1985). Even with limited continuity, these shales may act as baffles to fluid flow. The modeling of these compensational cycles is an important step in assessing the impact on the reservoir response to shale baffles and other related lithofacies trends.

The Data

The initial bathymetry is a fault-bounded, southwest-northeast–trending submarine depression, and it is assumed that seven vertical wells are available (Figure 7). Seven wells were chosen as a reasonably high level of conditioning in a typical deepwater reservoir study

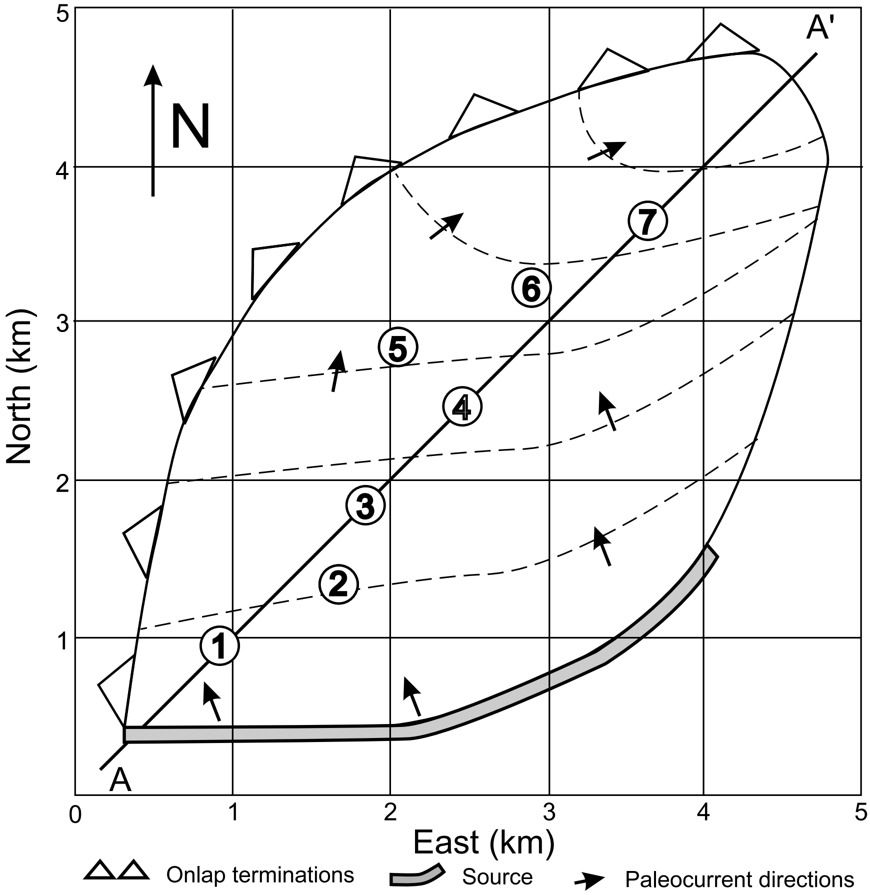

Figure 7. A schematic of the initial bathymetry loosely based on a study of Cengio turbidite system, Italy (Cazzolo et al., 1985). The dark-gray section represents the source for flow events. The fan lobe onlaps a mudstone slope along the west, northwest, and north. The vertical well locations and the paleocurrents are indicated. The study area is 25 km^2 (9.6 mi^2). The location of long section AA′ is indicated.

of this areal extent. Note that this is conservative because this method performs faster with less conditioning because fewer geometries are rejected. The contacts of the flow events were positioned along the wells with a similar density observed in the Cazzolo et al. (1985) case study. Porosity and permeability along the wells were generated synthetically such that porosity and permeability are correlated and have spatial correlation. The porosity and permeability data distributions are shown in Figure 8, and the scatter plot of permeability and porosity is shown in Figure 9.

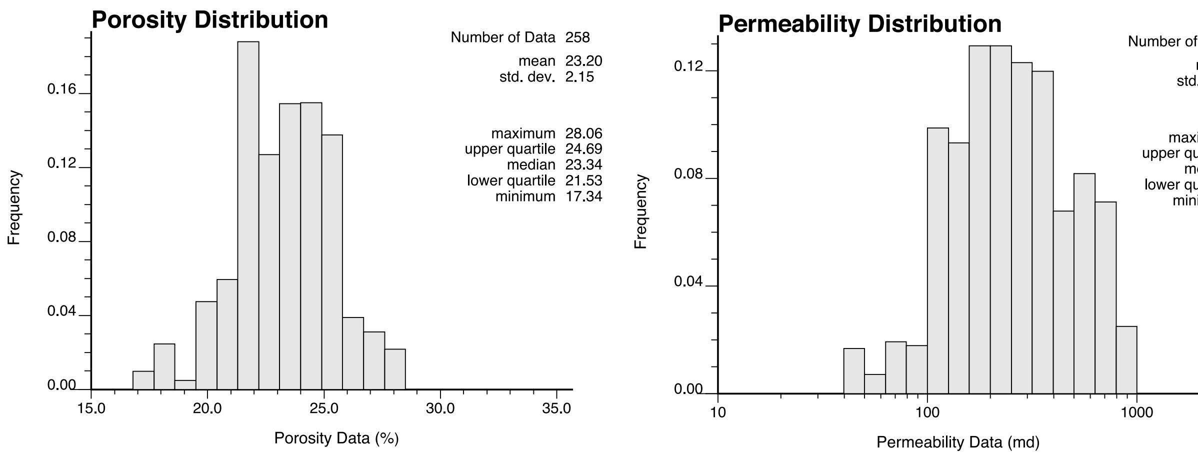

Figure 8. The distribution of porosity and permeability from synthetic well logs.

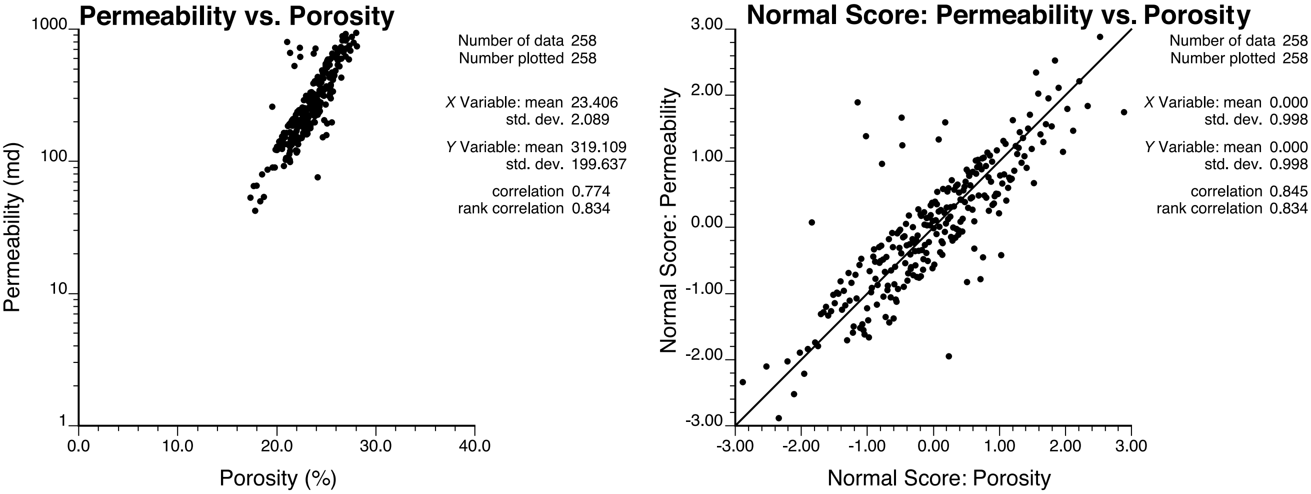

Figure 9. The scatterplots of well permeability and porosity before and after Gaussian transform. The permeability is in millidarcys, and the porosity is in percent.

Geostatistical Workflow

The application of stochastic surface-based simulation is demonstrated in a geostatistical workflow for the modeling of petrophysical properties in lobe VII. A common geostatistical workflow is to model (1) reservoir geometry, (2) lithofacies, and (3) petrophysical properties constrained by lithofacies. These models are conditional to all available data and analog information (Deutsch, 2002).

Model of Reservoir Geometry

Commonly, reservoir geometry is provided by seismic information calibrated to well logs. Seismic resolution is a function of the source frequency content, rock sonic properties, and the depth of the trace. With much of the three-dimensional architecture of the turbidite lobes below seismic resolution, there is commonly a significant level of uncertainty associated with respect to the reservoir geometry. This uncertainty may be carried through the stochastic workflow through the use of multiple reservoir geometry realizations or scenarios. These scenarios may be the result of simulated surfaces conditioned to well contacts or based on expert judgment of professional geologists. For each realization or scenario of reservoir geometry, a realization of facies and petrophysical properties may be calculated (M. J. Pyrcz, E. Gringarten, P. Frykman, and C. V. Deutsch, 2004, unpublished work). For this case study, only a single reservoir geometry was applied.

Lithofacies Models

Lithofacies types identified by Cazzolo et al. (1985) represent a range of reservoir quality from massive sandstone to mudstone. Significant trends in the facies exist, including (1) higher fraction of sandier amalgamated sandstones along the center axis, (2) fining to the distal, and (3) capping of sandy flows with mud drapes. It was decided not to explicitly model these lithofacies but instead constrain porosity and permeability by models that account for these lithofacies trends. Because the lithofacies represent a natural continuum from high-porosity and high-permeability sandstone to low-porosity and low-permeability mudstone, this substitution is reasonable.

Petrophysical Properties

The petrophysical properties, porosity and permeability, were modeled by the following steps: (1) calculate surfaces representing stochastic flow events in lobe VII; (2) construct a hierarchical trend model that characterizes the observed trends in lithofacies constrained to the surface-based model; (3) simulate porosity conditional to well log and hierarchical trend model as a local variable mean model (Deutsch and Journel, 1998); and (4) simulate permeability with the porosity realization as secondary data for collocated cokriging (Deutsch and Journel, 1998).

We recommend that a single realization of surface-based trend be coupled with a realization of porosity and permeability to produce a single reservoir realization, instead of a combination of matched trend and property realizations. The former is a more computationally efficient method to sample the model space of uncertainty and is applied in this case study (M. J. Pyrcz, E. Gringarten, P. Frykman, and C. V. Deutsch, 2004, unpublished work).

This methodology honors the available well-log porosity, permeability from log and core, the trend in the porosity and permeability given by geologic information on the transition in lithofacies, the geometry of flow event deposits, the compensational interrelationship of event deposits, and the relationship between porosity and permeability. The associated steps are demonstrated and discussed in detail.

Implementation of the methodology for generating stochastic flow event deposits for this specific case study requires the assignment of flow event geometric parameter distributions. The flow event geometric parameter distributions should be determined from well data and analog information. The size distributions should be consistent with the lobe geometry. If the distribution of flow event sizes is too small, then the distal section of the lobe may not be filled. In this case, the algorithm should be modified to allow for flow events disconnected from the source location.

For this case study, the parameter distributions were drawn from Gaussian and uniform distributions. The length of the flow event deposits L is drawn from a Gaussian distribution with mean of 5000 m (16,000 ft) and standard deviation of 1000 m (3300 ft). This parameter was set based on consistency with lobe VII. The length to the position of maximum width l is drawn from a uniform distribution of 40–70% of L; the maximum lobe width W is drawn from a uniform distribution of 10–30% of L; and the width of the source w is assigned as 40% of W. These areal geometric parameters result in a wide variety of lobe morphologies and reflect the uncertainty in their assignment given the limited areal information available in the outcrop study (Cazzolo et al., 1985). The width-to-height ratio was selected to reproduce the nominal flow event thickness of 1.0 m (3.3 ft) observed in the outcrop.

Two surface-based realizations were simulated, based on the reservoir geometry and the distribution of flow event parameters indicated above. The variogram of the stochastic residual was selected with a long range, and the amplitude was chosen as 0.5 m (1.6 ft). The first and second realizations are comprised of 121 and 71 flow events, respectively, as shown in long sections for two realizations (Figure 10). Each surface-based realization honors the identified contacts along the wells. Between the wells and at locations along the well with missing information, the realizations may vary greatly while honoring the flow event geometry and the compensational stacking pattern.

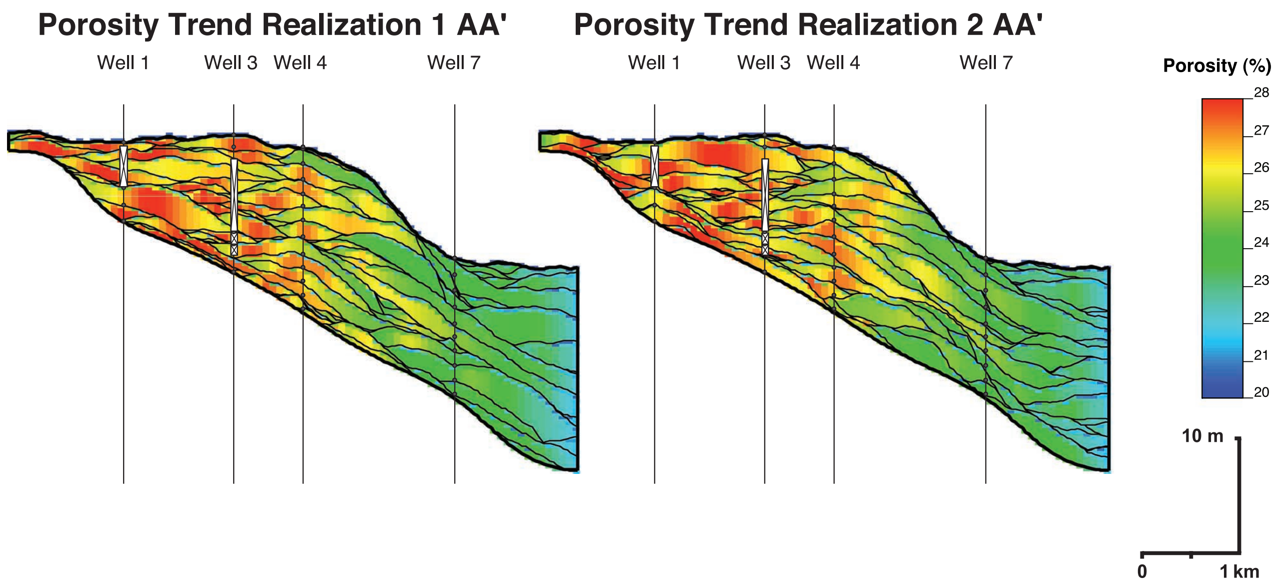

Figure 10. Two realizations of stochastic surfaces and associated porosity (percent) hierarchical trend models. The stochastic bounding surfaces of flow event deposits are shown as black lines. These surfaces are conditioned to contacts along the wells that are shown as black dots. The trends described in Figure 11 are reproduced, and the trend model mean is corrected to the mean porosity from the well logs.

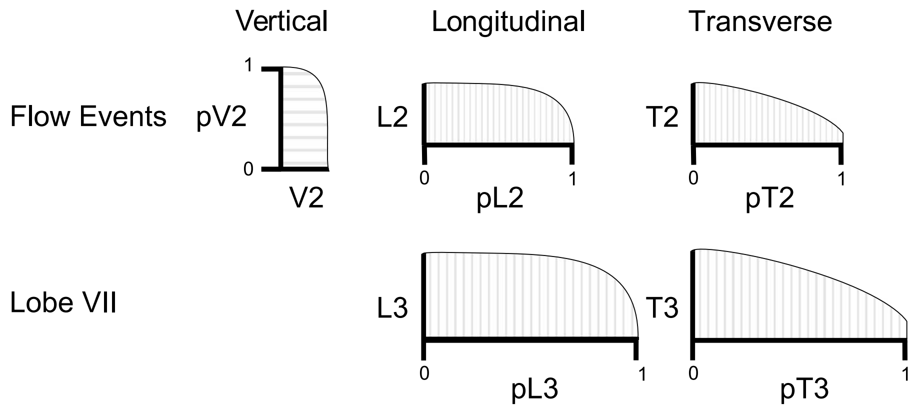

Figure 11. The porosity trends inferred from the lithofacies study of the Cengio turbidite system, Italy (Cazzolo et al., 1985). The flow events deposits may have subtle grading and are commonly capped by fine-grained facies. Flow events and the lobes demonstrate fining toward the distal and are coarsest along the primary axis of flow. pV2, pL2, pT2, pL3, and pT3 are the proportional coordinates in vertical, longitudinal, and transverse directions for the flow event deposits and the lobe. V2, L2, T2, L3, and T3 are associated the trend multiplier functions. No trend is identified in the vertical over the entire lobe.

The lithofacies trends were quantified as functions describing the trend in porosity (Figure 11). Mud drapes are represented by a sharp decrease in the porosity trend near the top of the flow events along with fining toward the peripheries as indicated in the longitudinal and transverse trend functions. The resulting hierarchical trend models based on the two surface-based simulations are shown in Figure 10, and a fence diagram of the first trend model is shown in Figure 12. The trend model integrates the complicated flow event deposits geometries and stacking pattern, while capturing trends such as fining distal, fining upward, and fining to the peripheries.

These trend models may be applied as local variable mean models for sequential Gaussian simulation (Deutsch and Journel, 1998) of porosity conditioned to well log. Sequential Gaussian simulation requires the modeling of semivariograms of the Gaussian transform of the data. The experimental semivariograms were calculated in the plane of the flow events (near horizontal) and orthogonal to the flow events (near vertical). The semivariograms were modeled by a spherical and a Gaussian nested structure (Figure 13).

Two realizations of porosity were calculated, each paired with a local variable mean model (Figure 10). These realizations reproduce the porosity conditioning from well log, the porosity distribution, and the porosity trends constrained to the stochastic surfaces (Figures 14, 15). At the sampled locations along the wells, the porosity realizations are the same, but away from

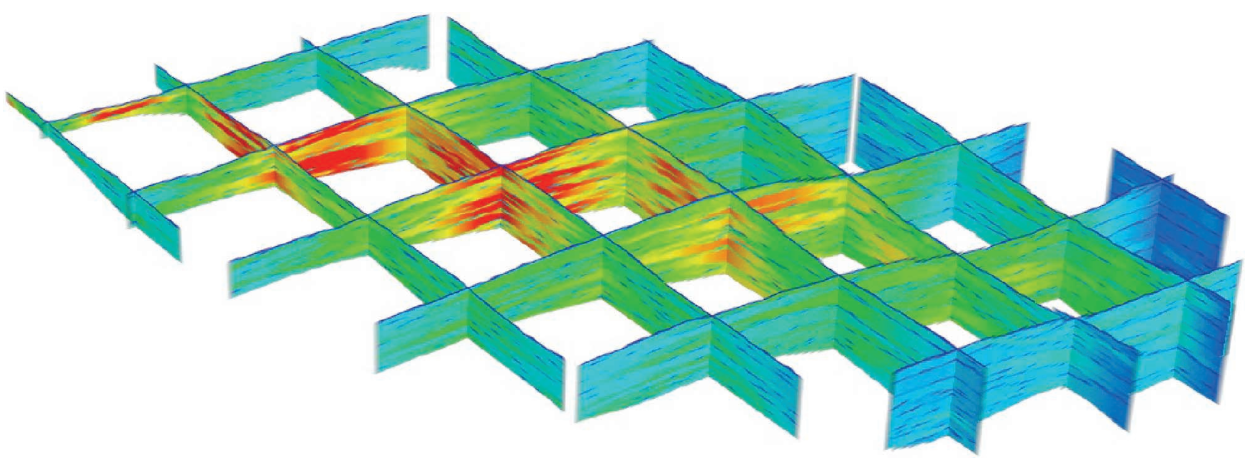

Figure 12. A fence diagram of the first realization of the porosity hierarchical trend model (30 × vertical exaggeration). Color scale is the same as in Figure 10.

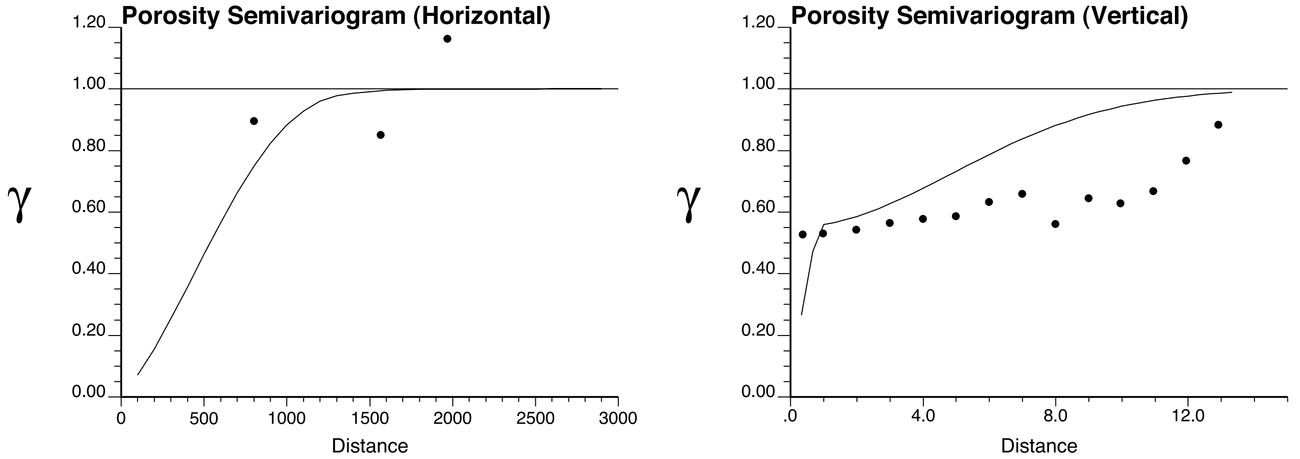

Figure 13. Horizontal and vertical semivariograms of the Gaussian transform of the porosity data.

the wells, the realizations may be quite different, while honoring the local variable trend model and stationary semivariogram.

The permeability distributions inferred from log and core available at the wells are shown in Figure 8. The correlation coefficient between the Gaussian transform of porosity and permeability may be inferred from the available conditioning (Figure 9) and from analog information. The experimental permeability semivariograms were calculated in the plane of the flow events (near horizontal) and orthogonal to the flow events (near vertical) (Figure 16).

Two realizations of permeability were simulated with the associated porosity realizations applied as collocated secondary data in a collocated cokriging context (Deutsch and Journel, 1998) (Figures 17, 18).

These realizations of reservoir petrophysical properties may be applied for reservoir development planning. These models may be subjected to flow simulation or other transfer functions. For example, ϕh maps may be calculated for each realization (Figure 19).

LIMITATIONS

Limitations exist with respect to the proposed surface-based technique:

- Adequate horizontal discretization is required. If the gradient in the bathymetry is high and the horizontal discretization is coarse, then sharp edges result at the peripheries of the flow events. In the

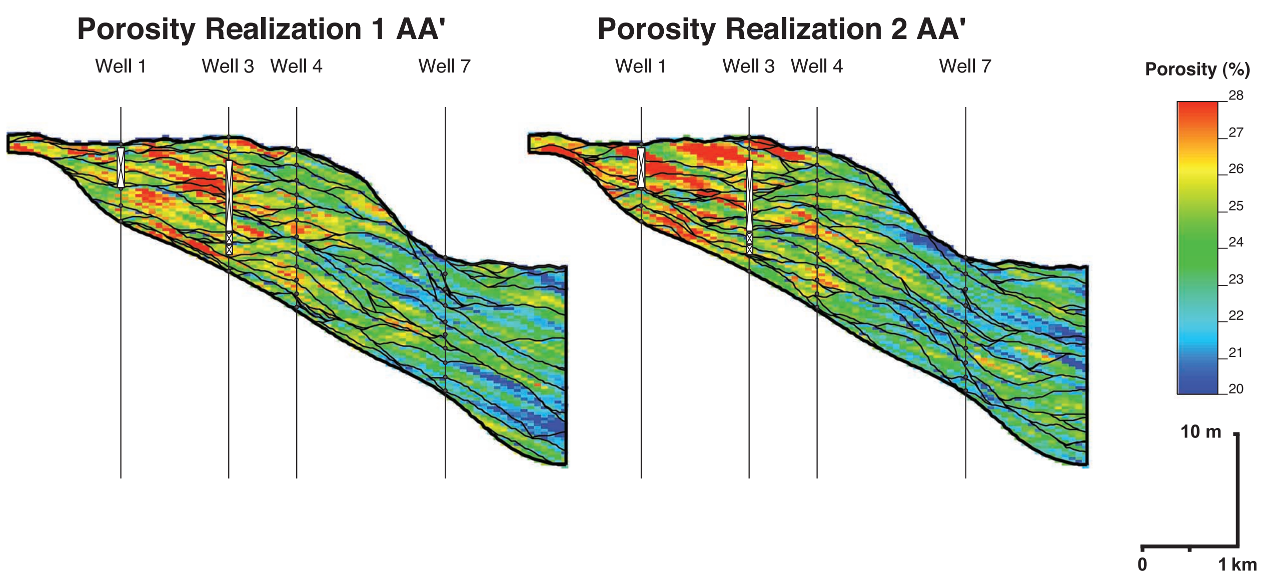

Figure 14. Two realizations of porosity constrained to the surface-based hierarchical trend model and conditioned to well logs.

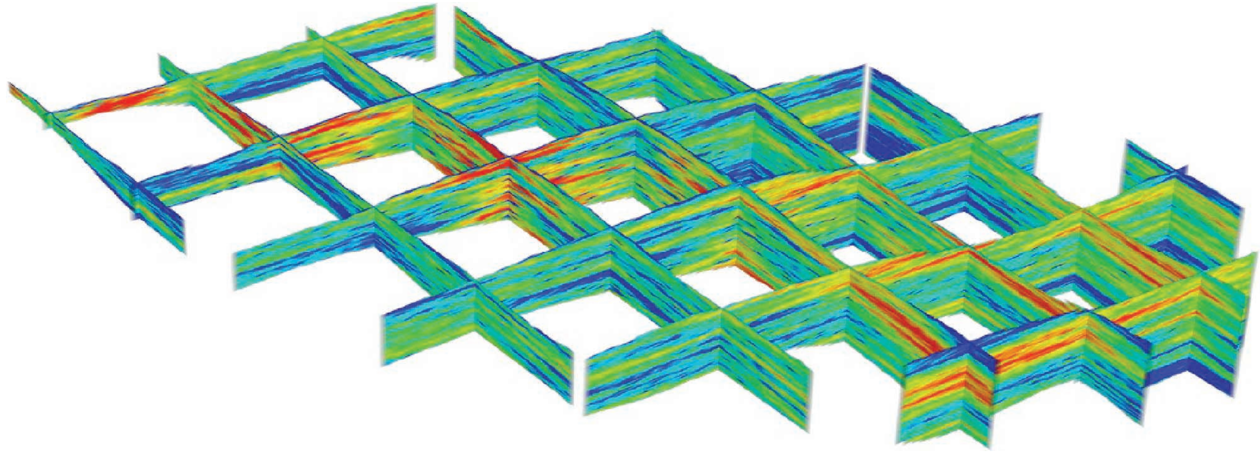

Figure 15. A fence diagram of the first porosity realization of the porosity hierarchical trend model (30 × vertical exaggeration). Color scale is the same as in Figure 14.

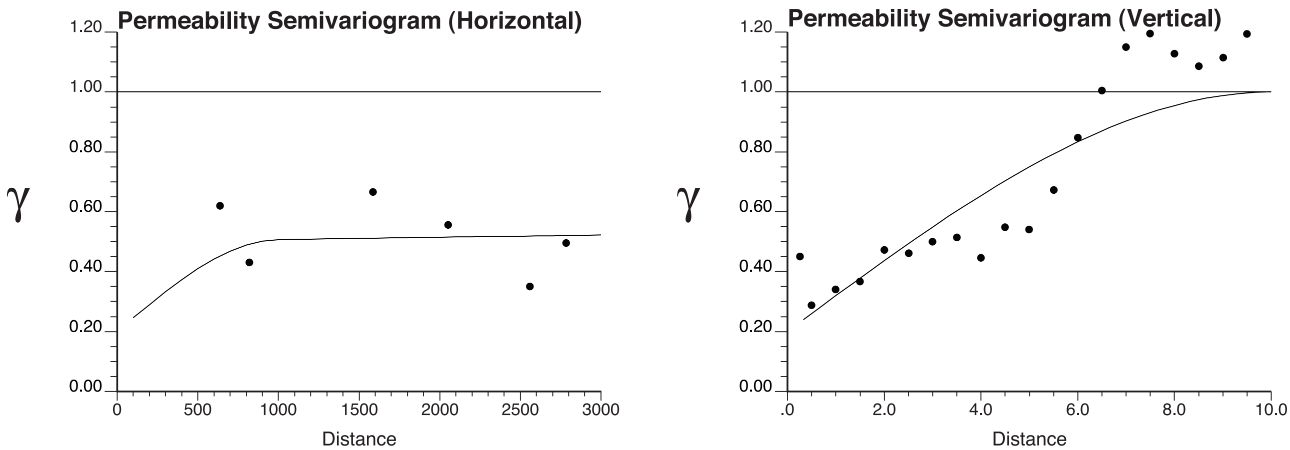

Figure 16. Horizontal and vertical semivariograms of the Gaussian transform of the permeability data.

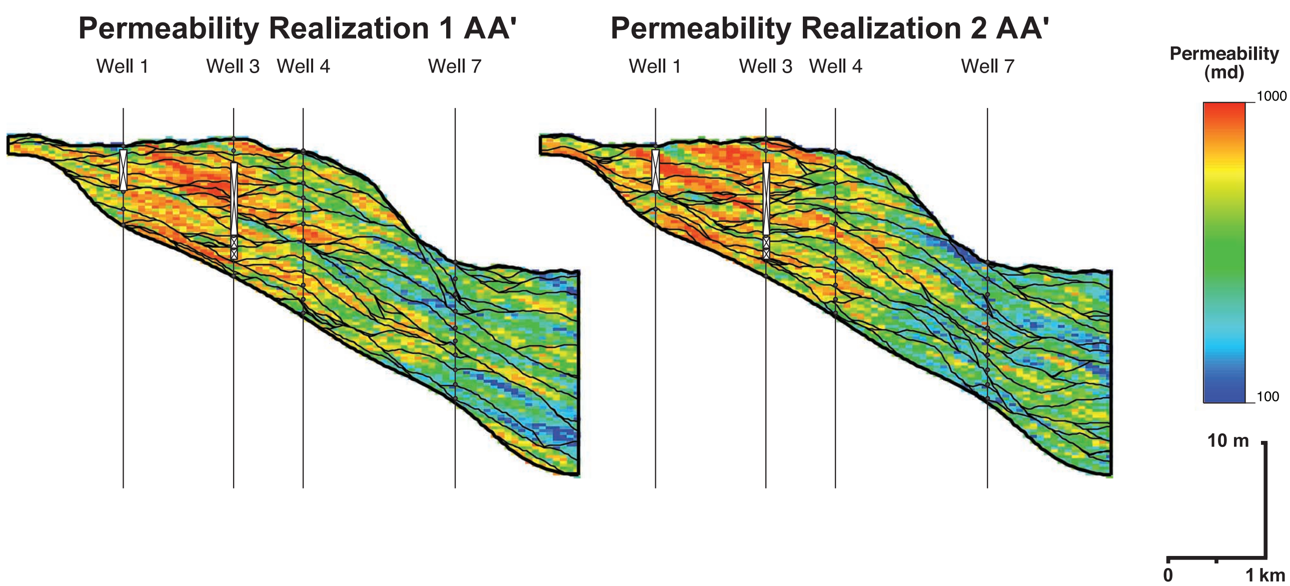

Figure 17. Two realizations of permeability correlated to the paired porosity realizations and conditioned to well logs (in millidarcys).

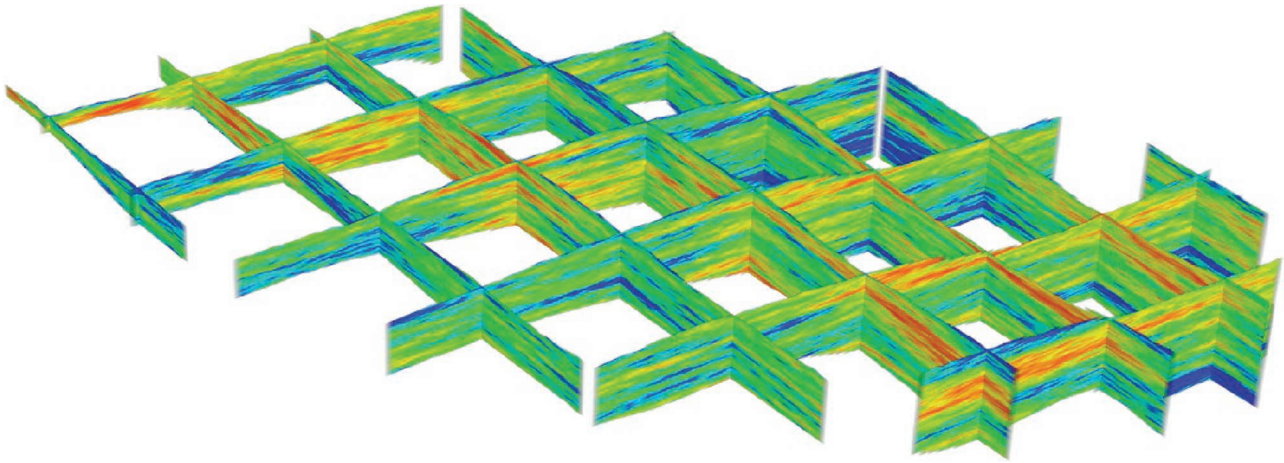

Figure 18. Fence diagram of the first permeability realization (30× vertical exaggeration). Color scale is the same as in Figure 17.

case study with a maximum gradient of about 1°, a 100 × 100 grid was applied without edge artifacts.

- As the level of conditioning increases or the flow event size increases, it is more difficult to match conditioning. This results in more rejected flow event geometries and, therefore, greater computational effort to calculate realizations. In this example, only about 20% of geometries were rejected, and less than 10 min was required for each realization.

CONCLUSIONS

A surface-based simulation algorithm is proposed that reproduces the geometries and compensational stacking patterns of flow event deposits in reservoir-scale turbidite lobes. The input parameters include original bathymetry, reservoir-scale lobe geometry, and geometric parameter distributions of the flow event deposits. The flow events respond to bathymetry by preferentially filling topographic lows and avoiding topographic highs.

This algorithm is demonstrated in a geostatistical workflow for the construction of stochastic turbidite lobe models that honor the available conditioning data, reproduce trends in petrophysical properties because of compensational cycles, and reproduce the relationship between porosity and permeability as characterized by the linear correlation coefficient. Multiple realizations of geometric and resulting trend models may be calculated to account for the uncertainty inherent to these small-scale features. These trend models are integrated in stochastic models to construct realistic

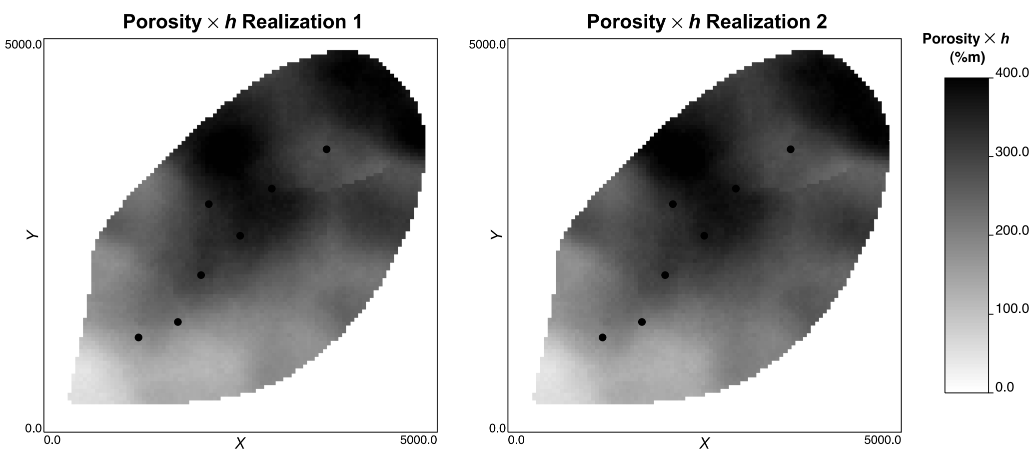

Figure 19. ϕh maps for two realizations of porosity.

turbidite reservoir lobe models that reproduce important geologic information and account for uncertainty with multiple realizations.

REFERENCES CITED

Alabert, F. G., and G. J. Massonnat, 1990, Heterogeneity in a complex turbiditic reservoir: Stochastic modeling of facies and petrophysical variability: Society of Petroleum Engineers Annual Technical Conference and Exhibition, New Orleans, Louisiana, p. 776–790.

Bouma, A. H., 1962, Sedimentation of some flysch deposits: A graphical approach to facies interpretation: New York, Elsevier, 168 p.

Bouma, A. H., 2000, Fine-grained, mud-rich turbidite systems: model and comparison with coarse-grained, sand-rich systems, *in* A. H. Bouma and C. G. Stone, eds., Fine-grained turbidite systems: AAPG Memoir 72/SEPM Special Publication 68, p. 9–20.

Cazzolo, C., E. Mutti, and B. Vigna, 1985, Cengio turbidite system, Italy, *in* A. H. Bouma, W. R. Normark, and N. E. Barnes, eds., Submarine fans and related turbidite systems: New York, Springer-Verlag, p. 179–183.

Cross, T. A., and J. W. Harbaugh, 1990, Quantitative dynamic stratigraphy: A workshop, a philosophy, a methodology, *in* T. A. Cross, ed., Quantitative dynamic stratigraphy: Eaglewood Cliffs, New Jersey, Prentice Hall, p. 3–20.

Deutsch, C. V., 2002, Geostatistical reservoir modeling: New York, Oxford University Press, 376 p.

Deutsch, C. V., and A. G. Journel, 1998, GSLIB: Geostatistical software library and users guide: New York, Oxford University Press, 369 p.

Deutsch, C. V., and T. T. Tran, 2002, FLUVSIM: A program for object-based stochastic modeling of fluvial depositional systems: Computers and Geosciences, v. 28, p. 525–535.

Deutsch, C. V., Y. Xie, and A. S. Cullick, 2001, Surface geometry and trend modeling for integration of stratigraphic data in reservoir models: 2001 Society of Petroleum Engineers Western Regional Meeting, March 26–30, Bakersfield, California, SPE Paper 68817.

De Vay, J. C., D. Risch, E. Scott, and C. Thomas, 2000, A Mississippi-sourced, middle Miocene (M4), fine-grained abyssal plain fan complex, northeastern Gulf of Mexico, *in* A. H. Bouma and C. G. Stone, eds., Fine-grained turbidite systems: AAPG Memoir 72/SEPM Special Publication 68, p. 109–118.

Dudley, P. R. C., D. E. Rehmer, and A. H. Bouma, 2000, Reservoir-scale characteristics of fine-grained sheet sands, Tanqua Karoo, South Africa, *in* P. Weimer, R. M. Slatt, J. Coleman, N. C. Rosen, H. Nelson, A. H. Bouma, M. J. Styzen, and D. T. Lawrence, eds., Deep-water reservoirs of the world: SEPM Gulf Coast Section Proceedings, 20th Annual Research Conference, p. 318–342.

Galloway, W. E., and D. K. Hobday, 1996, Terrigenous clastic depositional systems: New York, Springer, 489 p.

Ghosh, B., and D. R. Lowe, 1993, The architecture of deep-water channel complexes, Cretaceous Venado Sandstone Member, Sacramento Valley, California, *in* S. A. Graham and D. R. Lowe, eds., Advances in the sedimentary geology of the Great Valley Group, Sacramento Valley, California: SEPM Pacific Section, Special Publication, p. 51–65.

Haldorsen, H. H., and D. W. Chang, 1986, Notes on stochastic shales; from outcrop to simulation model, *in* L. W. Lake and H. B. Caroll, eds., Reservoir characterization: London, Academic Press, p. 445–485.

Haldorsen, H. H., and L. W. Lake, 1984, A new approach to shale management in field-scale model: Society of Petroleum Engineers Journal, April, p. 447–457.

Isaaks, E. H., and R. M. Srivastava, 1989, An introduction to applied geostatistics: New York, Oxford University Press, 561 p.

Johnson, S. D, F. Stephen, D. Hinds, and H. D. Wickens, 2001, Anatomy, geometry and sequence stratigraphy of basin floor to slope turbidite systems, Tanqua Karoo, South Africa: Sedimentology, v. 48, p. 987–1023.

Li, H., and C. D. White, 2003, Geostatistical models for shales in distributary channel point bars (Ferron Sandstone, Utah): From ground penetrating radar data to three-dimensional flow modeling: AAPG Bulletin, v. 87, p. 1851–1868.

Mutti, E., and W. R. Normark, 1987, Comparing examples of modern and ancient turbidite systems: Problems and concepts, *in* J. K. Legget and G. G. Zuffa, eds., Marine clastic sedimentology: Concepts and case studies: Boston, Graham and Trotman, p. 1–38.

Mutti, E., and W. R. Normark, 1991, An integrated approach to the study of turbidite systems, *in* P. Weimer and M. H. Link, eds., Seismic facies and sedimentary processes of submarine fans and turbidite systems: New York, Springer, p. 75–106.

Mutti, E., and M. Sonnino, 1981, Compensational cycles: A diagnostic feature of turbidite sandstone lobes (abs.): International Association of Sedimentologists, Second European Regional Meeting, Bologna Abstracts, p. 120–123.

Nilsen, T., and E. Abbate, 1985, Gottero turbidite system, Italy, *in* A. H. Bouma, W. R. Normark, and N. E. Barnes, eds., Submarine fans and related turbidite systems: New York, Springer-Verlag, p. 199–204.

Pickering, K. T., J. D. Clark, R. D. A. Smith, R. N. Hiscott, F. Ricci Lucchi, and N. H. Kenyon, 1995, Architectural element analysis of turbidite systems, and selected topical problems for sand-prone deep-water systems, *in* K. T. Pickering, R. N. Hiscott, N. H. Kenyon, F. Ricci Lucchi, and R. D. A. Smith, eds., Atlas of deepwater environments: Architectural style in turbidite systems: London, Chapman, and Hall, p. 1–10.

Pyrcz, M. J., 2004, The integration of geologic information into geostatistical models: Ph.D. in Mining Engineering, University of Alberta, Edmonton, 296 p.

Pyrcz, M. J., and C. V. Deutsch, 2003, Stochastic surface modeling in mud rich, fine-grained turbidite lobes (abs.): AAPG Annual Meeting, May 11–14, Salt Lake City, Utah, Extended abstract, www.searchanddiscovery.com/documents/abstracts/annual2003/extend/7796, 6 p.

Reading, H. G., and M. Richards, 1994, Turbidite systems in deep-water basin margins classified by grain size and feeder system: AAPG Bulletin, v. 78, p. 792–822.

Satur, N., A. Hurst, B. T. Cronin, G. Kelling, and K. Gurbuz, 2000, Sand body geometry in a sand-rich, deep-water clastic system, Miocene Cingoz Formation of southern Turkey: Marine and Petroleum Geology, v. 17, p. 239–252.

Shanmugam, G., 2000, 50 years of the turbidite paradigm (1950s–1990s): Deep-water processes and facies models— A critical perspective: Marine and Petroleum Geology, v. 17, p. 285–342.

Slatt, R. M, G. H. Brown, R. J. Davis, G. R. Clemenceau, J. R. Colbert, R. A. Young, H. Anxionnaz, and R. J. Spang, 1998, Outcrop-behind outcrop characterization of thin-bedded turbidites for improved understanding of analog reservoirs: New Zealand and Gulf of Mexico: Society of Petroleum Engineers

Annual Technical Conference and Exhibition, New Orleans, Louisiana, SPE Paper 49563, 8 p.
Stow, D. A. V., and M. Johansson, 2000, Deep-water massive sands: Nature, origin and hydrocarbon implications: Marine and Petroleum Geology, v. 17, p. 145–174.
Stow, D. A. V., and M. Mayall, 2000, Deep-water sedimentary systems: New models for the 21st century: Marine and Petroleum Geology, v. 17, p. 125–135.
Stow, D. A. V., H. G. Reading, and J. D. Collinson, 1996, Deep-seas, *in* H. G. Reading, ed., Sedimentary environments: Processes, facies and stratigraphy: London, Blackwell Science, p. 395–453.
Stoyan, D., W. S. Kendall, and J. Mecke, 1987, Stochastic geometry and its applications: New York, John Wiley & Sons, 345 p.
Strebelle, S., and K. Payrazyan, 2002, Modeling of a deepwater turbidite reservoir conditional to seismic data using multiple-point geostatistics: Society of Petroleum Engineers Annual Conference, San Antonio, Texas, SPE Paper 77425, 10 p.